Progress In Electromagnetics Research B, Vol. 31, 89–115, 2011

COMPARISONS OF IMPROVEMENTS ON TIME-DOMAIN TRANSMISSION WAVEFORM AND EYE DIAGRAM FOR FLAT SPIRAL DELAY LINE BETWEEN TWO TYPES GUARD TRACES IN HIGH-SPEED DIGITAL CIRCUITS

G.-H. Shiue* **and J.-H. Shiu**

Department of Electronic Engineering, Chung Yuan Christian University, 200, Chung Pei Road, Chung Li, Taoyuan 32023, Taiwan, R.O.C.

Abstract—This paper investigates the use of the guard traces to improve the Time-Domain Transmission (TDT) waveform and eye diagram for a flat spiral delay line. Two types of guard trace are adopted to implement and analysis in microstrip line and stripline structures. One is Two Grounded Vias type Guard Trace (TGVGT) and the other is Open-Stub type Guard Trace (OSGT). The time-domain analysis results by HSPICE and the associated simple circuit modeling is presented. According to the simulation results, the original TDT crosstalk noises can be reduced by about 80% when using TGVGTs or OSGTs in a stripline structure and by about 60% when using TGVGTs in a microstrip line structure. Additionally, the eye diagrams also can obtain improvement. The crosstalk noise cancelation mechanisms of the flat spiral routing scheme on TGVGTs and OSGTs are investigated by graphic method. In addition, how the degradation for the OSGT inserted into the flat spiral delay line in microstrip structure is clearly investigated. A flat spiral delay line inserted into TGVGTs and OSGTs both can obtain good improvements of the TDT waveform and eye diagram in a stripline structure. Moreover, adding OSGTs to the flat spiral routing scheme is easily accomplished due to the open end of OSGTs. Finally, HSPICE simulation and time-domain measurements of crosstalk noises of TDT waveforms, and eye diagrams are use to validate the proposed structure and analysis.

Received 17 April 2011, Accepted 26 May 2011, Scheduled 4 June 2011

* Corresponding author: Guang-Hwa Shiue (ghs@cycu.edu.tw).

1. INTRODUCTION

As the cycle time of a computer system enters the sub-nanosecond range, the fraction of cycle time needed to accommodate clock skew for synchronization of the clock signal among logic gates increases. While several schemes have been developed that minimize clock skew, delay lines are typically employed in the critical nets of packages or Printed Circuit Boards (PCBs). In general, in high-speed digital circuits the delay lines include the serpentine and flat spiral routing schemes as shown in Fig. 1. Intuitively, total time delay should be proportional to total length of the delay line. However, crosstalk noise induced by closely packed transmission lines accumulates at the receiving end, and may cause significant deterioration in total time delay and even result in false switching of logic gates [1–3].

Figure 1. Two typical routing schemes for the delay line. (a) Serpentine routing scheme. (b) Flat spiral routing scheme.

Guard traces, which are conductor lines grounded by a few plated via holes, are utilized to diminish crosstalk noise between adjacent conductor paths in PCBs, or packages. However, crosstalk reduction is constrained by certain design parameters [4–7]. A microstrip serpentine delay line with the guard traces inserted into the cross-coupled conductors in the parallel section has been proposed to improve delay line frequency characteristics [8]. Improvements on the transient transmission waveform and eye diagram of a serpentine delay line using guard traces have been studied [9, 10]. The inserted guard traces with only two grounded vias at both ends can reduce crosstalk noise interferences at the received end of the serpentine delay line in a microstrip structure. The noise cancellation mechanisms of near-end and far-end crosstalk noise interferences on the TGVGTs in a microstrip line structure have been presented [10]. Another guard trace type, i.e., one with a grounded via at one end and the other end, which is open (i.e., OSGT), has been used to reduce crosstalk at the receiving end in a stripline structure. Additionally, a previous work has elucidated the noise cancellation mechanism of near-end crosstalk noise on the OSGTs in strip line structure [11]. However, to our knowledge, crosstalk noise reduction for a flat spiral delay line using guard traces

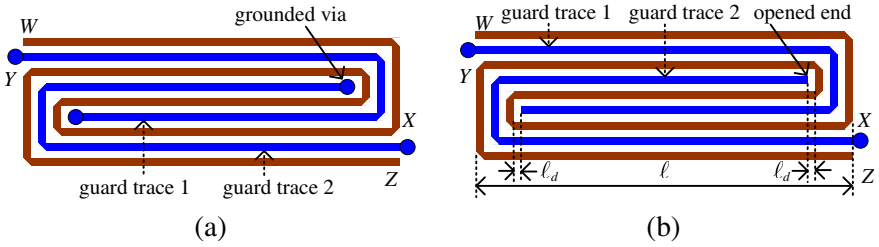

Figure 2. Two types of inserted guard trace scheme for the flat spiral delay line. (a) Two grounded vias type guard trace. (b) Open-stub type guard trace.

has not been studied.

Although the flat spiral delay line has better signal integrity than a serpentine delay line at the receiving end, the transient transmission waveform also has some crosstalk noise [3]. For high-speed compact digital circuit, the crosstalk noise still degrades the transient transmission waveform and eye diagram of a flat spiral delay line. Thus, two guard traces, the TGVGT and OSGT as shown in Fig. 2, are adopted to reduce the crosstalk on transient transmission waveform and eye diagram for a flat spiral delay line in microstrip and stripline structures. Additionally, the noise cancellation mechanisms of near-end and far-end crosstalk noise interferences on TGVGTs for a microstrip line and near-end crosstalk noise on the OSGTs for the strip line, respectively, also occur in a flat spiral delay line. However, due to the flat spiral routing scheme, this work investigates incomplete noise cancellation that does not exist in a serpentine delay line. A graphic method is adopted to investigate the noise cancellation mechanisms. Moreover, this work demonstrates that the inserted OSGTs and TGVGTs both obtain good improvements for a flat spiral delay stripline.

The organization of this paper is as follows. Section 2 investigates coupled microstrip lines and striplines with inserted TGVGTs or OSGTs to understand the crosstalk effects of these two guard traces Section 3 constructs the HSPICE circuit model for a flat spiral delay line with guard traces. TDT waveforms and eye diagrams for a flat spiral delay line with and without TGVGTs and OSGTs in the microstrip line and stripline structures are compared. Subsequently, the crosstalk noise cancellation mechanism on OSGTs is clearly explained by graphic method. Moreover, additional OSGTs or TGVGTs can both obtain the good improvements to the TDT waveform and eye diagram of a flat spiral delay stripline. Simulation

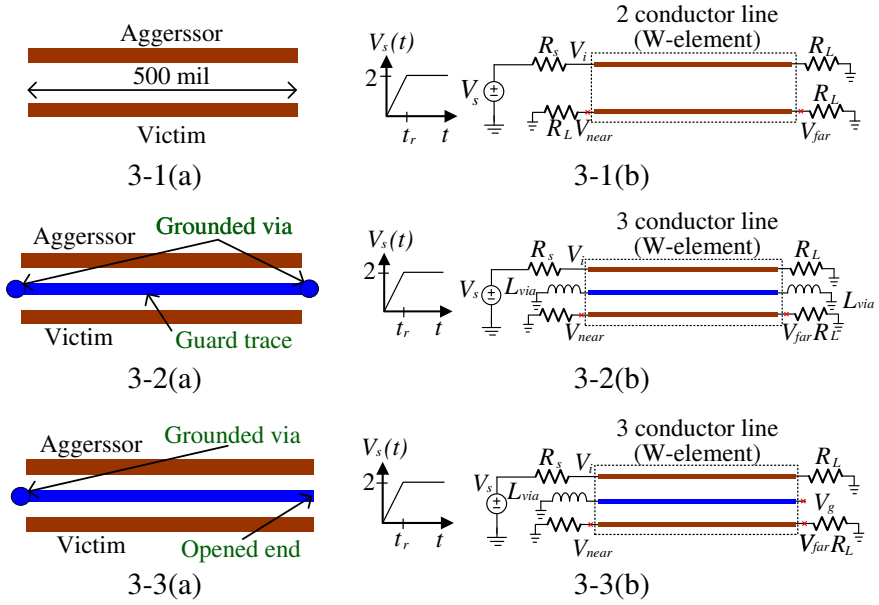

Figure 3. (a) Top views and (b) equivalent HSPICE simulation circuits of the coupled lines with and without guard traces. Fig. 3-2 is the coupled lines with TGVGT and Fig. 3-3 is the coupled lines with OSGT.

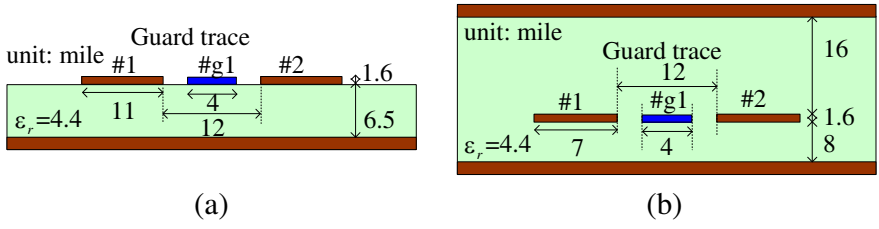

Figure 4. Cross-sectional view of the coupled lines inserted guard trace with geometrical dimensions and material. (a) Microstrip structure. (b) Stripline structure.

and measurement results between measured eye diagrams for different conditions are compared for verification in Section 3. Conclusions are given in Section 4.

2. COUPLED LINES WITH GUARD TRACES

Guard traces are commonly utilized to diminish crosstalk noise between adjacent conductor paths in PCBs or packages. Two guard traces, TGVGT and OSGT, are proposed. Fig. 3-1(a) shows typical coupled lines without a guard trace and with the TGVGT shown in Fig. 3-2(a) and OSGT shown in Fig. 3-3(a). Fig. 4 shows the cross-sectional views of the coupled microstrip lines and striplines. In addition, Fig. 4 depicts all geometric dimensions and material, e.g., trace width, spacing between coupled lines, trace thickness, substrate height and dielectric constant.

Under the assumption of weak coupling in the coupled transmission lines as shown in Fig. 3-1(a), the main signal in the active line is rarely affected by the crosstalk noise. Then, with respect to input voltage, V_i voltage magnitudes of saturated near-end and far-end crosstalk levels in the victim line can be formulated as [12]

$$V_{near} = V_i \times k_{near} = V_i \times \frac{1}{4}\left(\frac{L_m}{L_S} + \frac{C_m}{C_S}\right) \tag{1}$$

$$V_{far} = -V_i \frac{t_d}{t_r} \times k_{far} = -V_i \times \frac{t_d}{2t_r}\left(\frac{L_m}{L_S} - \frac{C_m}{C_S}\right) \tag{2}$$

where L_m is mutual inductance, L_S is self-inductance, C_m is mutual capacitance, C_S is self-capacitance, t_d is line delay time, t_r is rise time, k_{near} is the near-end crosstalk coefficient, and k_{far} is the far-end crosstalk coefficient. However, in a homogenous environment such as a stripline, the far-end crosstalk coefficient is almost about zero; thus, far-end crosstalk voltage should approach zero. Further, if the guard trace can be regarded as an ideal grounding line, crosstalk coefficients can be reduced, as can crosstalk noise [10].

Figure 3 shows the top views of coupled lines with and without a guard trace structure and equivalent HSPICE simulation circuits. The multiple coupled transmission lines, as well as the guard traces, are modeled using W-element, which accounts for finite transmission line loss. The driver and load resistances, R_S and R_L, are chosen as matched impedance, and rise time (t_r) of the source, $V_S(t)$, is 50 ps. The grounded vias of OSGT and TGVGT are regarded as a series inductance [10]

$$L_{via} \approx \mu_0 \frac{h_{via}}{2\pi}\left[\ln\left(\frac{4h_{via}}{r_{via}}\right) + \frac{r_{via}}{h_{via}} - \frac{3}{4}\right] \tag{3}$$

where h_{via} and r_{via} are the height and radius of the grounded via, respectively.

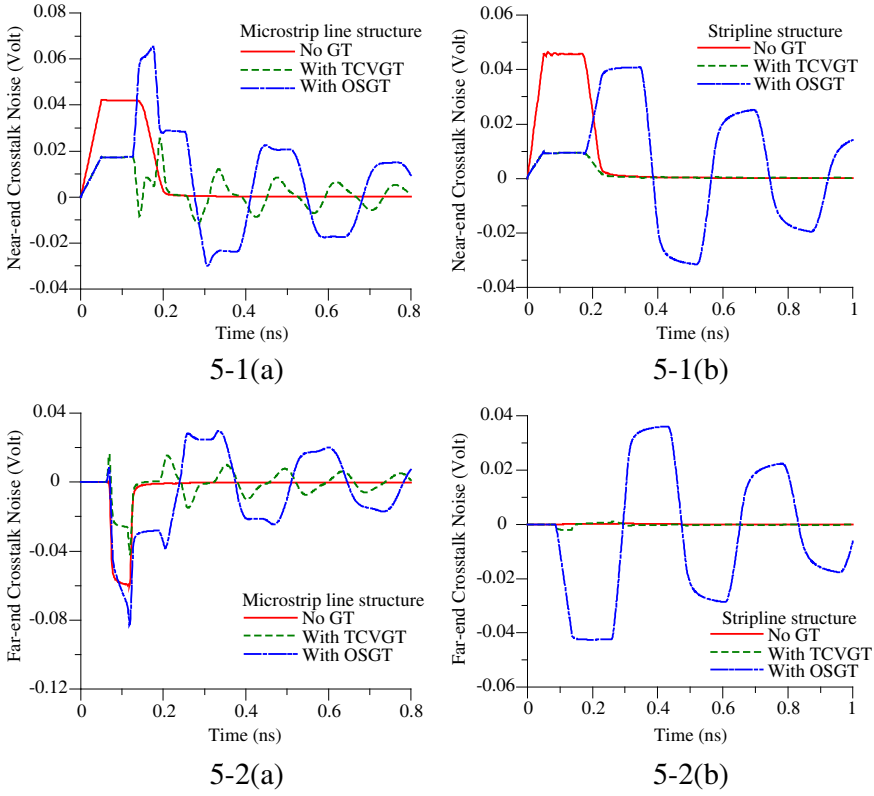

Figure 5. Figures 5-1(a) and 5-2(a) compare simulation results for near-end and far-end crosstalk noise for the coupled microstrip lines with and without guard traces. Figs. 5-1(b) and 5-2(b) compare simulation results for near-end and far-end crosstalk noise for the coupled striplines with and without guard traces.

Figures 5-1(a) and 5-2(a) compare simulation results for near-end and far-end crosstalk noise for coupled microstrip lines with and without guard traces, respectively. The coupled microstrip lines with an OSGT cannot reduce crosstalk noise and increase resonant crosstalk noise. In Fig. 6, the open-end voltage, V_g, induced by the aggressor line on OSGT in coupled microstrip lines is another noise source, which will add crosstalk noise to the victim line. In addition, for long coupled microstrip lines with an OSGT the far-end noise increases the peak voltage shown in Fig. 6 and the crosstalk noises increase at victim line. Further, with an additional TGVGT in the microstrip line structure, the resonant noises, also called ringing noise, exists in

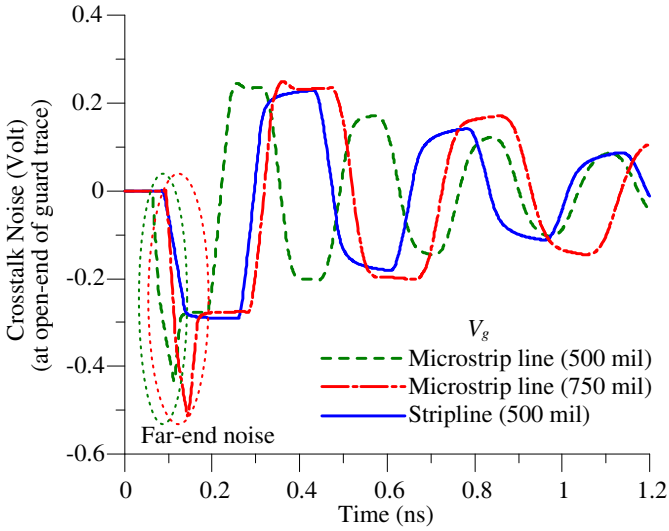

Figure 6. Comparison of the open-end voltage, V_g, of OSGT inserted in coupled lines. (a) Microstrip structure. (b) Stripline structure.

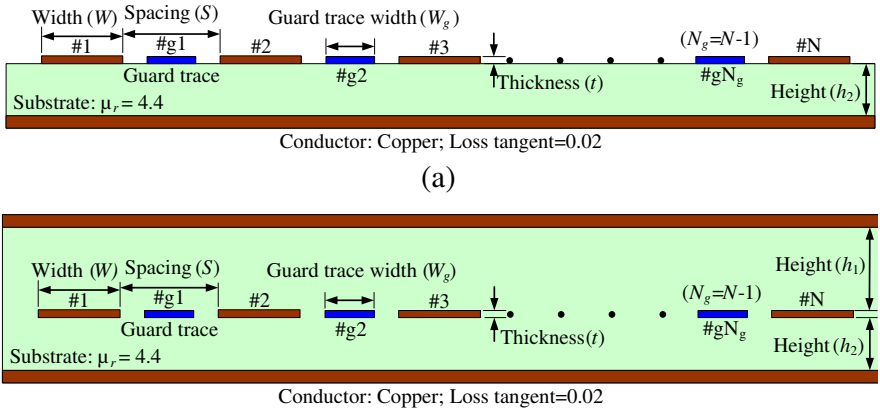

Figure 7. Cross-sectional view of the serpentine delay line with guard traces in reference to Fig. 2. (a) Microstrip structure. (b) Stripline structure.

crosstalk noise waveforms because the distance between two grounded vias is too far [13]. When the distance between two grounded vias increases, the guard trace may become another noise source on the

crosstalk noise waveforms. Hence, if the via separation is appropriate small, the resonant crosstalk noises can be reduced effectively [10].

Figures 5-1(b) and 5-2(b) compare the simulation results of near-end and far-end crosstalk noises for coupled striplines with and without guard traces, respectively. Obviously, the near-end crosstalk noise can be reduced significantly for coupled microstrip lines with a TGVGT. It is well known that the crosstalk noise only exited near-end crosstalk noise at near end of victim line in a stripline structure, a homogeneous environment [14]. However, the crosstalk noise still existed at the far-end of the victim line due to the open end for coupled striplines with an OSGT [15]. In Fig. 6, it can be found the open-end voltages on OSGT are large and resonant in stripline structures because the OSGT is a quarter-wavelength resonator. Therefore, near-end crosstalk noise induced by the aggressor line on the OSGT likes a noise source that causes a near-end crosstalk noise to the victim line.

Consequently, although the coupled lines inserted into an OSGT can obtain large crosstalk noises and bad signal integrity in microstrip line and stripline structures, the following analyses support the use of OSGTs to improve the transient transmission waveform more than when using TGVGTs for a flat spiral delay line in stripline structure.

3. FLAT SPIRAL DELAY LINE WITH GUARD TRACES

3.1. Flat Spiral Delay Line without Guard Traces

Consider a flat spiral delay line without guard traces formed by coupled lines shown in Fig. 1(b). It is known that the near-end crosstalk, V_{near}, among sections in a flat spiral delay line accumulates in phase appearing as flat wave noise on the TDT waveform and is twice the amplitude of near-end crosstalk as shown in Figs. 9 and 10. The maximum voltage of flat wave noise approximates by [2]

$$V_{flat,\max} = 2 \times V_{near}. \tag{4}$$

The accumulation of crosstalk noise degrades the TDT waveform and eye diagram.

3.2. Flat Spiral Delay Line with Guard Traces

Since the inserted guard traces can reduce near-end crosstalk among the sections in the serpentine delay line [9, 10], the flat spiral delay line with guard traces is also proposed to improve the maximum voltage of flat wave noise on the TDT waveform of a flat spiral delay line. The two guard traces, TGVGT and OSGT, are implemented.

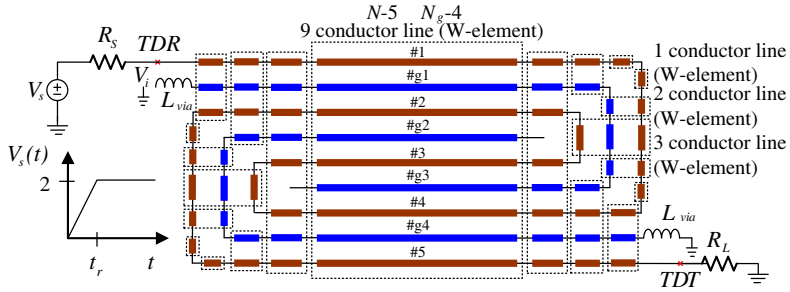

Figure 8. Circuit model for OSGTs inserted flat spiral delay line in HSPICE simulation. ($N = 5$).

Figure 2 shows the top views of two typical flat spiral delay lines formed by coupled lines with TGVGTs and OSGTs. The following analyses, consider the microstrip line and stripline structures. Fig. 7 shows the cross-sectional view of the flat spiral delay line, depicting all structural parameters — trace with (W), length (ℓ) of parallel traces, section number of the serpentine trace (N) ($N \geq 5$), separation between open end of OSGT and vertical trace (λ_d), section number of the guard trace (N_g) ($N_g = N - 1$), guard trace width (W_g), spacing between coupled lines (S), trace thickness (t), substrate height (h_1, h_2) $losstan = 0.02$, and dielectric constant (ε_r). The material and dimensional parameters of following simulated structures for a flat spiral delay line with and without guard traces are the same shown in Fig. 4. Separation λ_d is the same as signal trace width (W).

3.3. Circuit Modeling

Figure 8 shows the circuit model used in the HSPICE simulation for a flat spiral delay line with inserted guard traces. The multiple coupled transmission lines, as well as the guard traces, are modeled using W-elements, which accounts for the finite transmission line loss. Additionally, the vertical traces of the delay line are also modeled using W-elements. The discontinuity effect of mitered bends is neglected [16], because it influences the TDT waveform markedly less than crosstalk effects. The grounded via of guard traces is regarded as series inductance by formula (3). In HSPICE simulation, the driver and load resistances are $R_S = R_L = 50\,\Omega$ and rise time (t_r) of the source $V_S(t)$ is 50ps for TDT waveform simulation. In the following analysis examples, length (ℓ) of parallel traces is 500 mil and the section number of the serpentine trace (N) is 5. Further, using HSPICE and Designer [17] simulators, the pseudorandom incident signal is launched with rise/fall

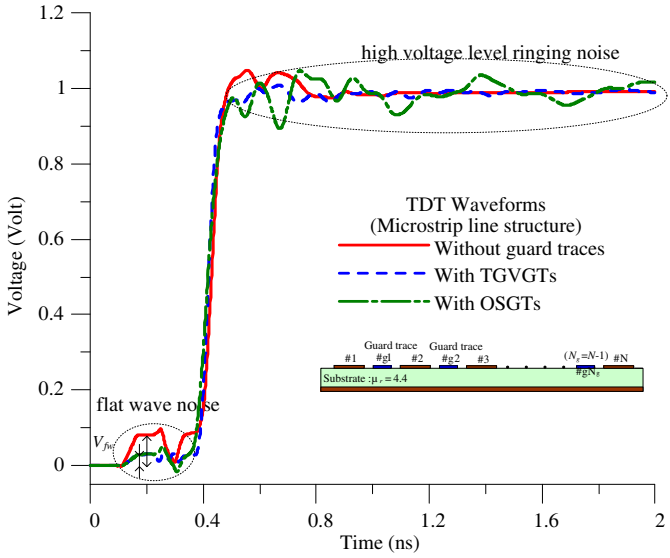

Figure 9. Comparison of TDT waveforms of the flat spiral delay line with and without guard traces in the microstrip line structure.

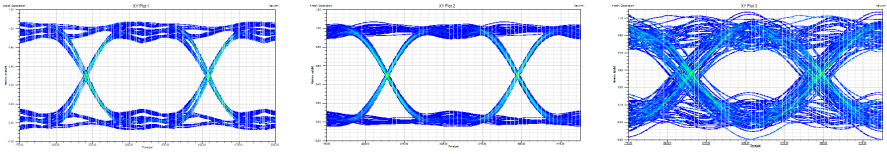

(a) (b) (c)

Figure 10. Comparison of eye diagram of the flat spiral delay line with and without guard traces in the microstrip line structure. (a) Without guard traces. (b) With TGVGTs. (c) With OSGTs.

time 50 ps, data rate of 6 Gb/s, and voltage swing of 2 V for eye diagram simulation.

3.4. Simulation and Analysis

Figure 9 compares of TDT waveforms of the flat spiral delay line with and without guard traces in microstrip line structure. Flat wave noise is reduced for the flat spiral delay line with both TGVGTs and OSGTs. However, a large ringing noise exists at the high voltage level of TDT waveform with additional OSGTs in the microstrip line structure. According to the investigations in Section 2, compared to

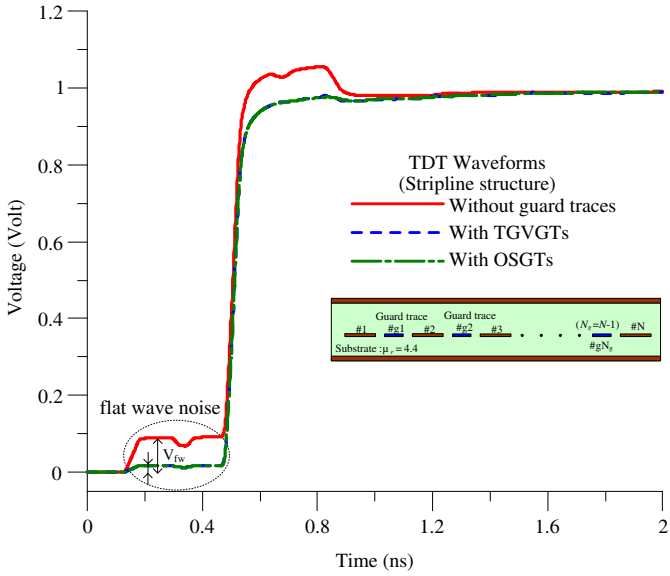

Figure 11. Comparison of TDT waveforms of the flat spiral delay line with and without guard traces in the stripline structure.

coupled lines without a guard trace and with an OSGT the amplitude of crosstalk noises increases at the near end and far end for coupled microstrip lines. Hence, the large ringing noise results from the near-end and far-end crosstalk noises on OSGTs induced by flat spiral trace. The induced crosstalk noises, V_{g2}, on the OSGTs can be shown in Fig. 13(a). Obviously, the larger crosstalk noise on guard trace is the amount of induced noise on the TDT waveform [14] is larger. Thus, the eye diagram of flat spiral delay line with OSGTs can be degraded significantly, as shown in Fig. 10 and Table 1. However, with additional TGVGTs in the microstrip line structure, no obvious ringing noise exists due to the crosstalk noise cancelation mechanism on TGVGTs [10]. The noise cancelation mechanism of TGVGTs in the flat spiral routing scheme is almost like the serpentine routing scheme with TGVGTs in the microstrip line structure. Thus, the TDT waveform and eye diagram of the flat spiral delay line with TGVGTs can also be improved, as shown in Figs. 9 and 10 and Tables 1 and 3. In Table 3, the TDT crosstalk noise of without guard traces can be reduced about 60% when using TGVGTs in the microstrip line structure.

Figures 11 and 12 and Tables 2 and 3 compare TDT waveforms and eye diagrams of a flat spiral delay line with and without guard

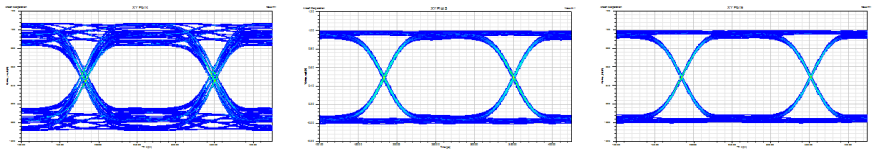

(a) (b) (c)

Figure 12. Comparison of eye diagram parameters of the flat spiral delay line with and without guard traces in the stripline structure. (a) Without guard traces. (b) With TGVGTs. (c) With OSGTs.

Table 1. Comparison of eye diagram parameters of the flat spiral delay line with and without guard traces in a microstrip line structure.

Microstrip line	NO GTs	With TGVGTs	With OSGTs
Eye high (Volt)	0.75	0.80	0.52
Eye width (Volt)	159	161	125
Jitter (ps)	8.37	6.85	67.02

Table 2. Comparison of eye diagram parameters of the flat spiral delay line with and without guard traces in the stripline structure.

Stripline	NO GTs	With TGVGTs	With OSGTs
EYE high (Volt)	0.49	0.78	0.79
Eye width (Volt)	146	162	163
Jitter (ps)	11.69	4.68	3.67

Table 3. Comparison of reduction ratios of flat wave noise amplitude between the flat spiral delay line with and without guard traces in microstrip line and stripline structures.

V_{fw} (mV)	NO GTs	With TGVGTs	Reduced ratio	With OSGTs	Reduced ratio
Microstrip line	81.8	29.6	63.8%	-	-
Stripline	89.5	16.9	81.1%	16.8	81.2%

traces in the stripline structure. Obviously, compared to no guard trace, the voltage levels of flat wave noise of TDT waveforms for flat spiral delay striplines with OSGTs and TGVGTs are both reduced significantly; the reduction ratios are about 80%. The two TDT

waveforms between the flat spiral delay stripline with OSGTs and TGVGTs are similar, as shown in Fig. 11. Hence, the eye diagrams of the flat spiral delay stripline with OSGTs and TGVGTs are both improved significant, as shown in Fig. 12 and Table 2.

It is well known that the far-end crosstalk noise can almost approach zero and thus be neglected in a stripline structure. In a stripline structure, crosstalk noise is only considered at the near end. Then, according to the investigations in Section 2, for coupled striplines with an OSGT, the crosstalk noise become large and appears at the near end and far end, as shown in Figs. 5-1(b) and 5-2(b). However, for the flat spiral routing scheme with the guard trace surrounded by the signal trace, it also exists the crosstalk noise cancelation mechanism that almost likes serpentine routing scheme on OSGTs [11] in a stripline structure. Hence, the voltage waveforms, V_{g1} and V_{g2}, on guard traces for a flat spiral delay stripline with OSGTs and TGVGTs are small, as shown in Fig. 13. Fig. 13 also shows the simulated voltage waveforms, V_{g1} and V_{g2}, on guard traces for a flat spiral delay line with OSGTs and TGVGTs obtained using CST, three-dimensional (3D) full-wave simulation based on the finite integration technique [18]. The results are similar to HSPICE simulation results. Good agreement validates the accuracy of the present equivalent circuit model. Because the voltage level of the two guard trace voltages, V_{g1}, of the flat spiral delay line with OSGTs and TGVGTs are small and differ minimally, the two TDT waveforms between the flat spiral delay stripline with additional OSGTs and TGVGTs are almost alike. Consequently, almost no resonant ringing noise exists at the high voltage level of TDT waveforms.

3.5. Noise Cancellation Mechanism

A popular graphic method based on wave tracing has been developed to illustrate and predict the crosstalk waveforms for two coupled transmission lines with matched termination [19]. By using the same graphic method, the noise cancellation mechanisms for flat spiral delay microstrip line and stripline with inserted OSGTs and TGVGTs can be illustrated as follows. The following illustration considers a circumstance in which the rise time is smaller than twice the delay time. To avoid confusion, Figs. 14 and 15 illustrate the wave tracing graphs of a flat spiral delay line with additional OSGTs and TGVGTs for near-end and far-end crosstalk noises, respectively. Additionally, in Fig. 2, the signal section $\overline{ABC}$ with guard trace 1 and the signal section $\overline{BCD}$ with guard trace 2 have almost the same noise cancellation mechanisms. For simplicity, Figs. 14 and 15 show only one part, $\overline{ABC}$ with guard trace 1.

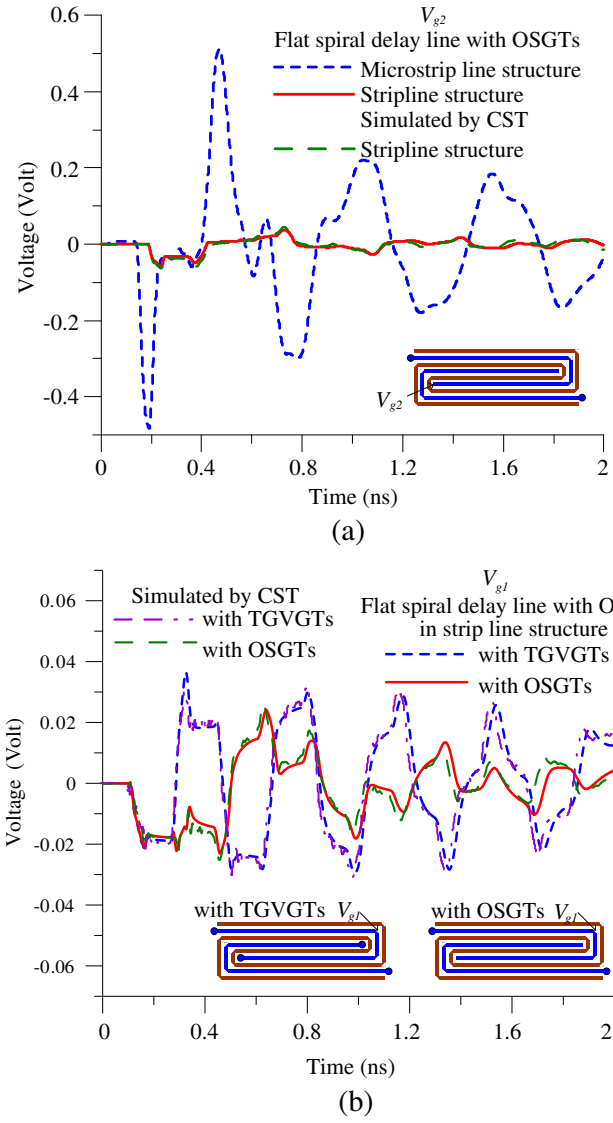

Figure 13. Comparisons of voltage waveforms on the guard trace for the flat spiral delay line with inserted guard traces.

3.5.1. Noise Cancellation Mechanism of Near-end Crosstalk Noise

Figure 14 summarizes the propagation of near-end crosstalk noise on the OSGT, Figs. 14(a), (b), (c), (d), and on TGVGT, Figs. 14(a), (b), (e), (f), respectively. Figs. 14(a), (b) illustrate

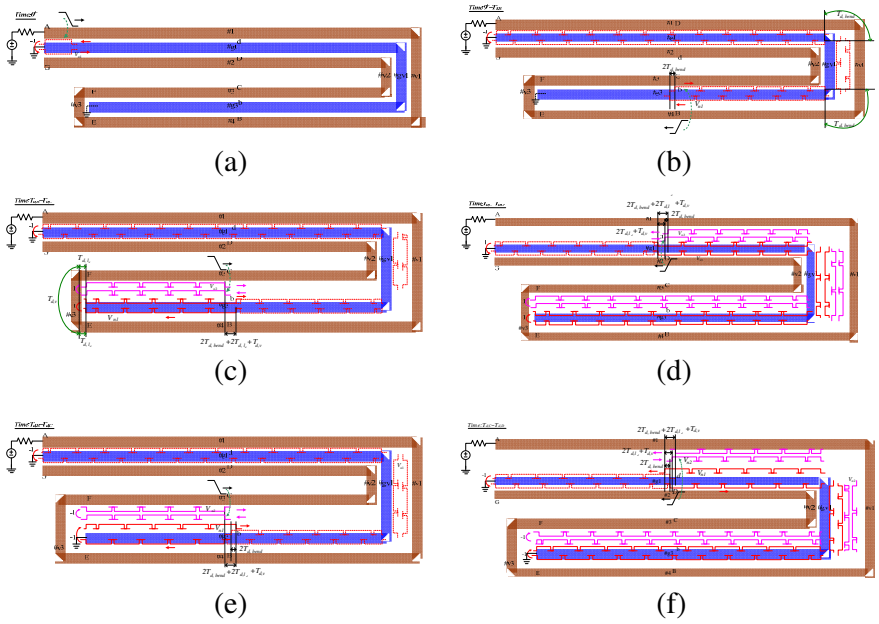

Figure 14. Summary of the propagation of near-end crosstalk noises on the OSGT ((a), (b), (c), (d)) and TGVGT ((a), (b), (e), (f)) #g1 at time intervals of (a) 0^+; (b) $0 \sim T_{d,B}$; (c)(e) $T_{d,B} \sim T_{d,C}$; (d)(f) $T_{d,C} \sim T_{d,D}$.

common situations for flat spiral delay line of additional OSGTs and TGVGTs. Moreover, to facilitate a description of Fig. 14, V_{n1} and V_{n2} denote the backward crosstalk noise coupling on the guard trace (#g1, #gv1, #g3) from the signal line $\overline{ABE}$ section and $\overline{FCDG}$ section, respectively. A ramped pulse propagating from position A along trace section #1 of the flat spiral delay line causes near-end crosstalk 1 (V_{n1}) to propagate towards the left end portion of the guard trace #g1. As V_{n1} propagates to the left end of guard trace #g1, noise is cancelled because the reflection coefficient is -1 (shorting via), as shown in Fig. 14(a). Next, V_{n1} inverts voltage polarity and propagates towards the right end portion of guard trace #g1 and through vertical section #vg1, and two bends arrival at position b. Almost simultaneously, the main signal still propagates along trace section #1 through vertical section #v1, and two bends arrive at position B. Owing to the time delay of two bends ($2T_{d,bend}$), V_{n1} is not cancelled completely, as shown in Fig. 14(b). The time difference, $2T_{d,bend}$, results in a small negative voltage waveform on V_{g2}, as shown in Fig. 13(a).

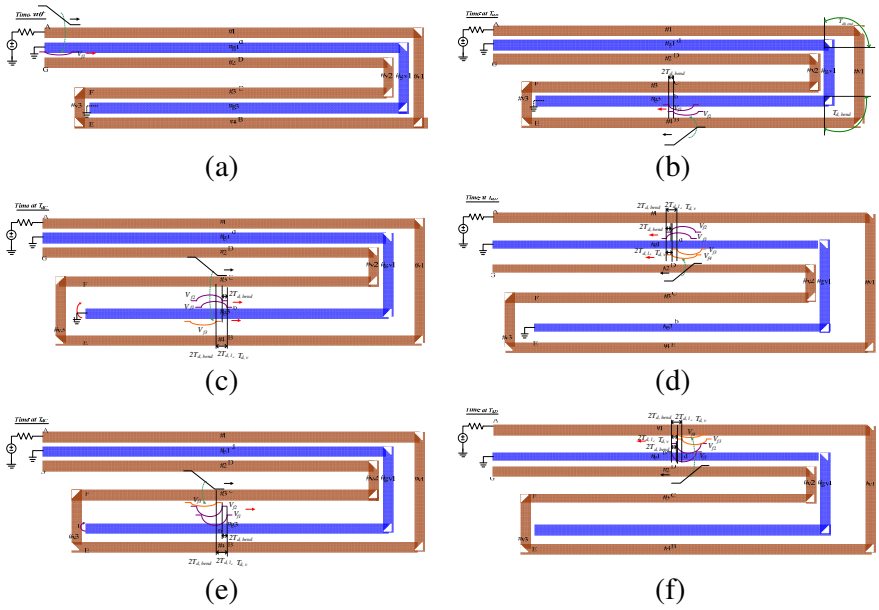

Figure 15. Summary of the propagation of far-end crosstalk noises on the TGVGT ((a), (b), (c), (d)) and OSGT ((a), (b), (e), (f)) #g1 at time intervals of (a) 0^+; (b) $T_{d,B}$; (c)(e) $T_{d,C}$; (d)(f) $T_{d,D}$.

Once arriving at the left end of #g3, V_{n1} encounters an open end (additional OSGTs condition) or short end (additional TGVGTs condition). Hence, the following time after V_{n1} arrives at the left end of #g3 is divided into two conditions (additional OSGTs and TGVGTs conditions) to introduce the following performance.

For additional OSGTs condition is shown as following. Because the left end portion of the guard trace section #g3 is open, V_{n1} maintains voltage polarity (negative polarity) and propagates towards the right end portion of guard trace section #g3. However, due to the flat spiral routing pattern, the ramped pulse arrives at the left end of trace section #4 and propagates through vertical section #v3 and along trace section #3 towards the right end, subsequently inducing near-end crosstalk noise 2 (V_{n2}) on the guard trace #g3. Notably, V_{n2} propagates towards the left end and encounters the open end of #g3. Next, V_{n2} maintains the voltage polarity (positive polarity) and propagates towards the right end portion of guard trace #g3. When the main signal arrives at position C, the time difference between the two near-end crosstalk noise interferences,V_{n1} and V_{n2}, is $2T_{d,bend} + T_{d,v} + 2T_{d,ld}$, as shown in Fig. 14(c). Consequently, the

main signal arrives at position D, and the amount of two crosstalk noise interferences that are incompletely canceled out due to the time differences of $2T_{d,bend}$, $2T_{d,bend}+T_{d,v}+2T_{d,ld}$ and $T_{d,v}+2T_{d,ld}$. Notably, the noise cancellation is incomplete owing to the three time differences of near-end crosstalk noises on OSGT, explaining why there is only a slight amount of noise interference on OSGT as shown in Fig. 13(b). Thereafter, the near-end crosstalk noise interference repeats the same action on the other OSGT.

For additional TGVGTs case, because it only the V_{n1} inverts voltage polarity (positive polarity) to propagate from the shorting end, as shown in Fig. 14(e), the other propagated performances like the additional OSGTs case. The detail descriptions are omitted in here. Consequently, when the main signal propagates through two bends and vertical trace arrives at position D, the two crosstalk noises also arrives at near position d, as shown in Fig. 14(f). The amount of the two crosstalk noise interferences canceled out is slightly diminished due to the time differences between $2T_{d,bend}$, $2T_{d,bend} + T_{d,v} + 2T_{d,ld}$ and $T_{d,v} + 2T_{d,ld}$. Interestingly, the noise cancellation is incomplete owing to the three time differences in near-end crosstalk noise interferences on TGVGT. Therefore, a slight amount of noise interference also occurs on TGVGT, as shown in Fig. 13(b). Thereafter, the near-end crosstalk noise interference repeats the same action on the other TGVGT.

3.5.2. Noise Cancellation Mechanism of Far-end Crosstalk Noise

Figure 15 summarizes the propagation of far-end crosstalk noise on OSGT, Figs. 15(a), (b), (c), (d), and on TGVGT, Figs. 15(a), (b), (e), (f), respectively. Figs. 15(a), (b) also reveal common situations for flat spiral delay line additional OSGTs and TGVGTs. To facilitate a description of Fig. 15, owing to the extremely small length of vertical parallel lines, its far-end crosstalk noise can be ignored in this graphic diagram. Additionally, V_{f1}, V_{f2}, V_{f3} and V_{f4} denote the far-end crosstalk noise interferences coupled on guard traces #g1 and #g3 from signal lines #1, #4, #3 and #2, respectively.

A situation in which a ramped pulse propagates from position A along trace section #1 of a flat spiral delay line causes V_{f1} to propagate towards the right end of the guard trace #g1, as shown in Fig. 15(a). Next, V_{f1} propagates through the vertical section #vg1, and the two bends arrive at position b. Almost simultaneously, the main signal still propagates along trace section #1 through vertical section #v1, and two bends and trace section #4 arrive at position B. When the main signal still propagates along trace section #4, V_{f2} is induced on #g3. Owing to the two bent trace sections, the time difference between the two far-end crosstalk noises, V_{f1} and V_{f2}, is $2T_{d,bend}$, as shown in

Fig. 15(b). Then, upon their arrival at the left end of #g3, V_{f1} and V_{f2} encounter an open end (an additional OSGTs condition) or short end (an additional TGVGTs condition). Hence, the next time after V_{f1} arrives at the left end portion of #g3 leads to the division into two conditions (additional TGVGTs and OSGTs conditions).

For additional TGVGTs condition is shown as following. Because the left end portion of the guard trace section #g3 is short to the ground, V_{f1} and V_{f2} invert the voltage polarity (positive polarity) and propagate towards the right end portion of guard trace section #g3. Simultaneously, when the main signal arrives at position C, the far-end crosstalk noise V_{f3} is induced on guard trace #g3, as shown in Fig. 15(c). The time delay between V_{f1} and V_{f3} is $2T_{d,bend}+T_{d,v}+2T_{d,ld}$. The three far-end crosstalk noise interferences then propagate through the vertical section #gv1 and guard trace section #g1 to the position d. Meanwhile, when the main signal arrives at position D, the far-end crosstalk noise V_{f4} is induced on guard trace #g3, as shown in Fig. 15(d). The time delay between V_{f1} and V_{f4} is $T_{d,v}+2T_{d,ld}$. Owing to slight time differences between the four far-end crosstalk noise interferences, the noise cancel effect is incomplete and the amplitude of the sum of the four far-end crosstalk noises is small, as shown in Fig. 16(a) under small ℓ.

However, Fig. 14 adequately explains the mechanism of near-end crosstalk noise cancellation of a flat spiral delay line that inserts OSGTs and TGVGTs in microstrip and stripline structures. Owing to far-end crosstalk noise almost only in a microstrip structure, the graphic explanations in Fig. 15 for additional OSGTs or TGVGT are used for a flat spiral delay only in a microstrip line structure. Based on the above graphic method, the amplitudes of voltage V_{g1} on guard trace for the flat spiral delay line with TGVGTs or OSGTs are both small, as shown in Fig. 13(b) due to the crosstalk noise cancellation mechanisms. Hence, with inserted TGVGTs or OSGTs the TDT waveforms and eye diagrams of the flat spiral delay stripline have nearly the same results, as shown in Figs. 11, 12 and Table 2.

For additional OSGTs case, due to the open ended, V_{f1} and V_{f2} maintain voltage polarity (negative polarity) and propagate from the shorting end to propagate, as shown in Fig. 15(e), the other propagated performances like the additional TGVGTs case. Those detail descriptions is omitted in here. When the main signal arrives at position D, far-end crosstalk noise V_{f4} is induced on guard trace #g3, as shown in Fig. 15(f). Notably, the time delay between V_{f1} and V_{f4} is $T_{d,v} + 2T_{d,ld}$. Also, the amplitude of the sum of the four far-end crosstalk noise interferences is large, as shown in Fig. 15(f). The simulated result is shown in Fig. 13(a). Furthermore,

Table 4. Comparison of the maximum magnitudes of the ringing noise on TDT waveform of a flat spiral delay line with TGVGTs in microstrip line structure.

	V_{ring_max} (mV)
Approach Formula (5)	56
HSPICE Simulation	53 (lossless)
	45 (with loss)

the large amplitude of the far-end crosstalk noise interferences on OSGTs degrades the TDT waveform and eye diagram of a flat spiral delay line in the microstrip line structure, as shown in Figs. 9, 10(c). Consequently, no noise cancellation mechanism is found in the additional OSGTs case.

Based on the above graphical explanations, since the open end of OSGTs causes the reflected waves to maintain their voltage polarity, all of the induced far-end crosstalk noises have the same polarity, and the far-end crosstalk noise on the OSGTs cannot be canceled. In contrast, the shorting via of TGVGTs causes the voltage polarity of the reflected waves to be inverted, so all of the induced far-end crosstalk noise has various voltage polarities and cancels out. Consequently, the OSGTs cannot be used in a microstrip structure.

The noise cancellation mechanism with incomplete cancellation also cancels two types of crosstalk noise, near-end crosstalk noise and far-end crosstalk noise for a flat spiral delay line with TGVGTs in the microstrip structure as shown in above section. It is well known that the far-end crosstalk noise is proportioned to the length of parallel traces in a microstrip line structure. Therefore, the parallel traces of the flat spiral delay line are long, and the induced far-end crosstalk noise on TGVGTs increases. Therefore, the voltage V_{g1} on TGVGTs is proportioned to the length of parallel traces, as shown in Fig. 16(a). The large voltage V_{g1} on TGVGTs results in a large ringing noise at the high voltage level and the early low voltage level of the TDT waveform with additional OSGTs in the microstrip line structure, as shown in Fig. 16(b). Consequently, using TGVGTs to improve the TDT waveform and eye diagram of the flat spiral delay line in the microstrip line structure is that the length of parallel traces can not two long.

Based on the crosstalk noise generation mechanism on TDT waveform [2, 3] and ringing noise induced by a guard trace on near-end crosstalk waveform [13], the maximum ringing noise, V_{ring_max}, at the high voltage level and the early low voltage level of the TDT

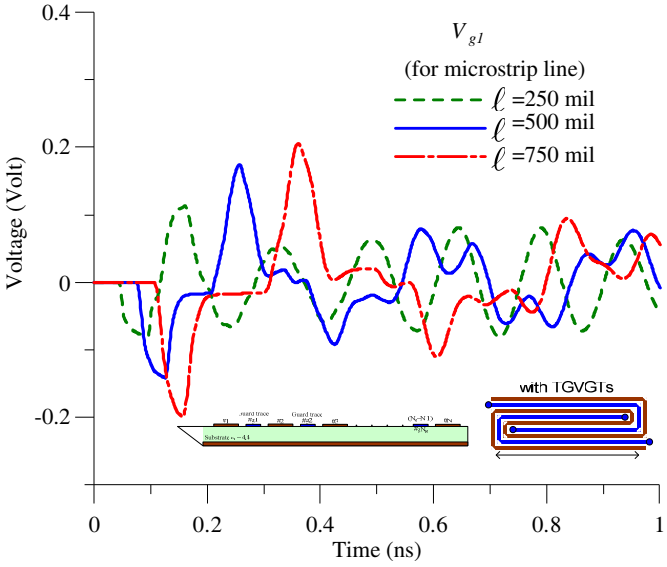

(a)

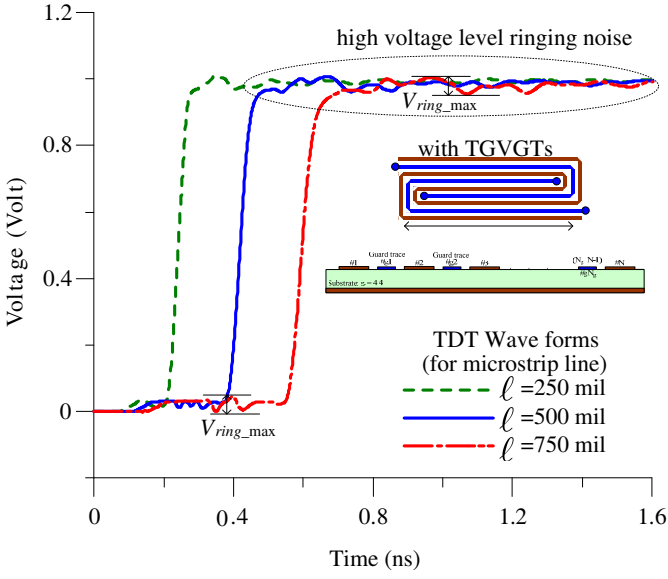

(b)

Figure 16. Comparison of (a) guard trace voltage, V_{g1}, and (b) TDT waveforms for the flat spiral delay line with inserted TGVGTs with different lengths.

Table 5. Comparison of the magnitudes of the crosstalk noise in TDT waveforms between the flat spiral and serpentine delay lines with/without TGVGTs/OSGTs in stripline structure.

$N = 7$	NO GTs	With TGVGTs/OSGTs
V_{fw} (mV)	89.5	16.8
$V_{iw,\max}$ (mV)	283	46.8

Table 6. Comparison of the measured eye diagram parameters of the flat spiral delay line with and without guard traces in the stripline structure.

Stripline	NO GTs	With TGVGTs	With OSGTs
Eye high (mV)	149	163	167
Eye width (mV)	136	150	154.5
Jitter (ps)	20.4	16.2	12.6

waveform are almost the same approach. The maximum magnitude of the ringing noise, $V_{ring\_\max}$, can be approached as [13]

$$V_{ring\_\max} \cong \frac{1}{4\sqrt{2}} V_i \frac{\ell_g}{v \times t_r} \left| \frac{L_{m,g}}{L_{s,g}} - \frac{C_{m,g}}{C_{s,g}} \right| = \frac{1}{4\sqrt{2}} V_i \frac{\ell_g}{v \times t_r} \left| k_{far,g} \right| \quad (5)$$

where ℓ_g is the length of guard trace, v is the velocity of noise on guard trace, and $k_{far,g}$ is the far-end crosstalk coefficient between the signal line and guard trace. Moreover, length (ℓ) of parallel traces of a flat spiral delay line, as shown in Fig. 2, is approaching $0.5\ell_g$. Consequently, the design guideline of maximum length ($\ell_{\max}$) of parallel traces of a flat spiral delay line can be approached as

$$\ell_{\max} \cong 2\sqrt{2} \frac{v \times t_r}{|k_{far,g}|} \frac{V_{ring\_\max}}{V_i}. \quad (6)$$

Table 4 compares the maximum magnitudes of the ringing noise on TDT waveform of a flat spiral delay line with TGVGTs in a microstrip line structure. Although the approached value of the maximum magnitude of the ringing noise by formula (5) is large than that of HSPICE simulation, using the approach formula (6) can obtain a strict and safe estimated design.

Figure 17 compares the TDT waveforms of the flat spiral and serpentine delay striplines with/without TGVGTs/OSGTs. Table 5 shows the magnitudes of the crosstalk noise in the TDT waveforms, shown presented in Fig. 17, for the flat spiral and serpentine delay lines with/without TGVGTs/OSGTs in the stripline structure. All structures have the same geometrical and material parameters as in the previous cases in Section 3.4, except for the number of sections (N). In the case without guard traces, the flat spiral routing delay line causes less crosstalk noise in the TDT waveform than does the serpentine routing scheme, because the amplitude of the flat wave noise produced by the flat spiral delay line is only double that of the near-end crosstalk noise that is induced between two coupled lines and the amplitude of the laddering wave noise induced by the serpentine delay line is $N-1$ times that of the near-end crosstalk noise [1–3]. In cases with additional guard traces, TGVGTs and OSGTs, the crosstalk noise in the TDT waveforms generated by each of two delay lines is significantly reduced, as shown in Fig. 17 and Table 5. However, since the amplitude of the flat wave noise generated by flat spiral delay line is still only the twice that of the near-end crosstalk, the flat spiral delay line with guard traces generates less crosstalk noise on the TDT waveform for a given number of sections ($N > 3$).

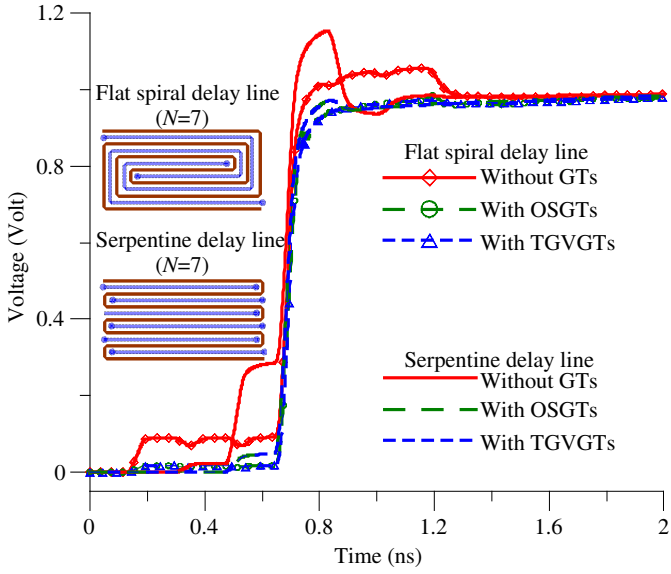

Figure 17. Comparison of TDT waveforms of the flat spiral and serpentine delay striplines between with/without TGVGTs/OSGTs.

4. EXPERIMENTAL VALIDATION

To verify that the proposed structure improves time-domain transmission waveforms and eye diagrams for flat spiral delay stripline the TDT waveforms are measured and compared with simulation results. The eye diagrams are also measured for comparison. To manufacture easily in a school laboratory, the five-section flat spiral delay line has the following cross-sectional parameters shown in Fig. 7(b): $W = 1\,\text{mm}$, $S = 1.5\,\text{mm}$, $W_g = 0.5\,\text{mm}$, $h_1 = 2.4\,\text{mm}$, $h_2 = 0.8\,\text{mm}$, $t = 0.035\,\text{mm}$, $\ell = 20\,\text{mm}$, $\varepsilon_r = 4.4$, and $losstan = 0.02$. Three different flat spiral delay striplines are manufactured — the original flat spiral delay stripline, a flat spiral delay stripline with TGVGTs and a flat spiral delay stripline with OSGTs.

The experiment is performed on the time-domain reflectometry TEK/CSA8000. With source and load resistances of $50\,\Omega$, the launching voltage source is drawn out of the reflectometry for HSPICE simulation. Fig. 18 compares the simulated and measured waveforms for guard traces inserted into a flat spiral delay stripline with TGVGTs or with OSGTs. It is evident that the simulated waveforms agree well with measured waveforms. Moreover, by using TGVGTs or OSGTs, the voltage level of flat wave noise on TDT waveforms is reduced significantly.

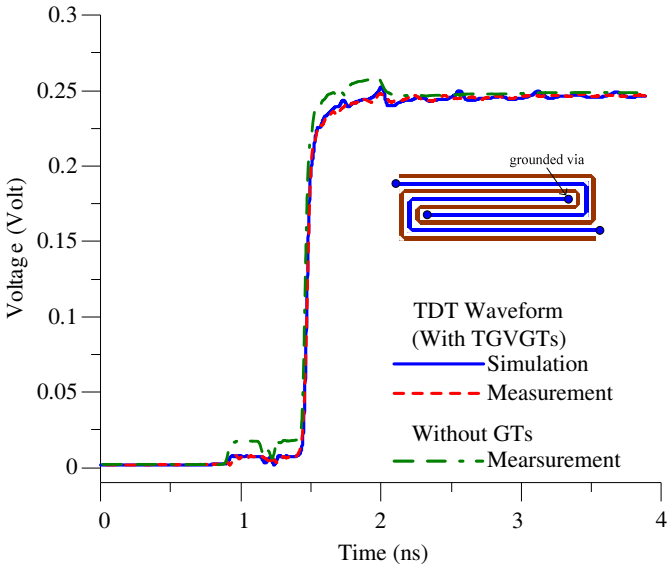

(a)

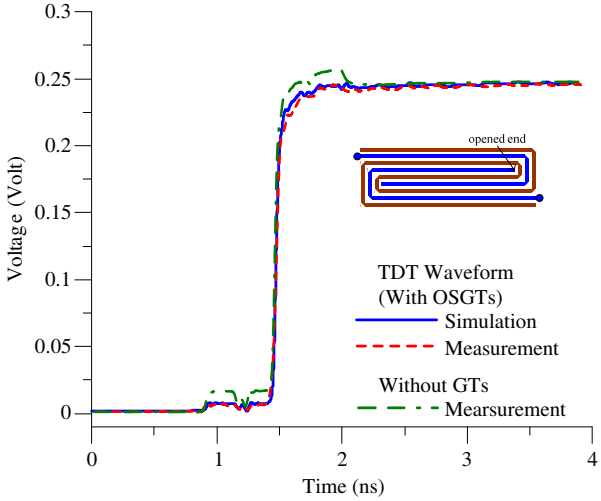

Figure 18. Comparison of simulated and measured TDT waveforms of the flat spiral delay line with and without guard traces in the stripline structure. (a) With TGVGTs. (b) With OSGTs.

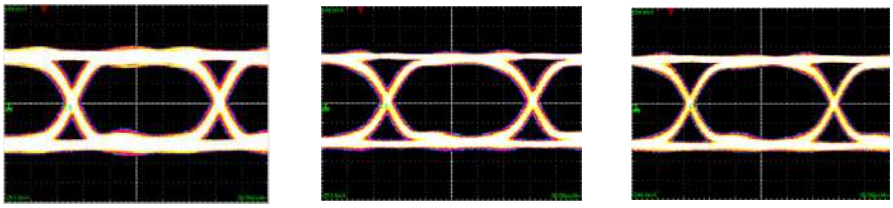

Figure 19. Comparison of the measured eye diagrams of flat spiral delay line with and without guard traces in the stripline structure. (a) Without guard traces. (b) With TGVGTs. (c) With OSGTs.

Figure 19 shows the comparison of measured eye diagrams between the flat spiral delay stripline with and with guard traces. Experimental verification is performed on the time-domain pattern generator Anritsu/MP1763C and oscilloscope Agilent/548855A. The launching pseudorandom voltage source has a rise time of 50 ps, voltage amplitude 0.25 volt, and data rate 6 Gbps. In Fig. 19 and Table 6, the eye diagrams can be improved for the flat spiral delay stripline with TGVGTs or with OSGTs.

5. CONCLUSION

This work uses guard traces to improve the time-domain transmission waveform and eye diagram for a flat spiral delay line. Two different guard traces, the TGVGT and the OSGT, are implemented and analyzed in microstrip line and stripline structures. A simple circuit modeling of time-domain analysis by HSPICE is presented. The TDT crosstalk noises without guard traces case can be reduced by about 80% when using TGVGTs or OSGTs in a stripline structure and by about 60% when using TGVGTs in a microstrip line structure. Furthermore, eye diagrams are also improved. The graphical illustrations clearly elucidate the noise cancellation mechanisms for a flat spiral delay line with TGVGTs or OSGTs in a spiral delay line AND stripline structure and with TGVGTs in a microstrip structure, respectively. Additionally, the mechanism of degradation that occurs when OSGT is inserted into the flat spiral delay line in a microstrip structure is examined. Despite the improved performance of a flat spiral delay line in a microstrip line structure when using TGVGTs, the length of parallel traces must be checked by the proposed formula. Additionally, with inserted TGVGTs or OSGTs, the TDT waveforms and eye diagrams of the flat spiral delay stripline have nearly the same good improvements, mil scale PCB especially. In addition, placing OSGTs inside the flat spiral routing scheme in stripline structure is easily accomplished due to the open end. Finally, HSPICE simulation and time-domain measurements of crosstalk noise in TDT waveforms and eye diagrams validate the proposed structure and analysis.

ACKNOWLEDGMENT

The authors would like to thank the NTUEE EDAPS Lab and Ansoft Taiwan for providing the measurement equipment and simulation software. This work was jointly supported in part by the National Science Council, Republic of China, under Grant NSC 98/99-2221-E-033-014, CYCU-EECS, under Grant CYCU-EECS-9903 and MPI Corporation, under Grant 99-09-03.

REFERENCES

1. Wu, R. B. and F. L. Chao, "Laddering wave in serpentine delay line," *IEEE Trans. Comp., Packag., Manuf. Technol. B*, Vol. 18, 644–650, Nov. 1995.
2. Wu, R. B., "Flat spiral delay line design with minimum crosstalk

penalty," *IEEE Trans. Comp., Packag., Manuf. Technol. B*, Vol. 19, 397–402, May 1996.

3. Guo, W. D., G. H. Shiue, and R. B. Wu, "Comparison between serpentine and flat spiral dealay lines on tranaient reflection/transmission waveforms and eye diagrams," *IEEE Trans. Microwave Theory Tech.*, Vol. 54, 1379–1387, Apr. 2006.
4. Ladd, D. N. and G. I. Costache, "SPICE simulation used to characterize the crosstalk reduction effect of additional tracks grounded with vias on printed circuit boards," *IEEE Trans. Circuits Syst. II*, Vol. 39, 342347, Jun. 1992.
5. Novak, I., B. Eged, and L. Hatvani, "Measurement by vector-network analyzer and simulation of crosstalk reduction on printed circuit boards with additional center traces," *Proc. IEEE Instrument Measurement Technol.*, 269–274, Irvine, CA, May 1993.
6. Li, Z., Q. Wang, and C. Shi, "Application of guard traces with vias in the RF PCB layout," *Proc. IEEE Int. Symp. Electromagnetic Compat.*, 771–774, May 2002.
7. Suntives, A., A. Khajooeizadeh, and R. Abhari, "Using via fences for crosstalk reduction in PCB circuits," *Proc. IEEE Int. Symp. Electromagnetic Compat.*, 34–37, Aug. 2006.
8. Nara, S. and K. Koshiji, "Study of delay time characteristics of multi-layered hyper-shield meander line," *Proc. IEEE Int. Symp. Electromagnetic Compat.*, 760–763, Aug. 200.
9. Shiue, G. H., C. Y. Chao, W. D. Guo, and R. B. Wu, "Improvement of time-domain transmission waveform in serpentine delay line with guard traces," *Proc. IEEE Int. Symp. Electromagnetic Compat.*, 1–5, Jul. 2007.
10. Shiue, G. H., C. Y. Chao, and R. B. Wu, "Guard trace design for improvement on transient waveforms and eye diagrams of serpentine delay line," *IEEE Trans. Adv. Packag.*, Vol. 33, No. 4, 1051–1060, Nov. 2010.
11. Shiue, G. H., J. H. Shiu, P. W. Chiu, Z. H. Zhang, M. N. Yeh, and W. C. Ku, "Improvements of time-domain transmission waveform and eye diagram of serpentine delay line using guard trace stubs in stripline structure," *2010 IEEE-EPEPS*, 249–252, Auxtin, TE, Oct. 24–27, 2010.
12. Feller, A., H. R. Kaupp, and J. J. Digiacomo, "Crosstalk and reflections in high-speed digital systems," *Proc. Fall Joint Comput. Conf.*, 512–525, 1965.
13. Cheng, Y. S., W. D. Guo, G. H. Shiue, H. H. Cheng, C. C. Wang,

and R. B. Wu, "Fewest vias design for microstrip guard trace by using overlying dielectric," *2008 IEEE-EPEP*, 321–324, San Jose, CA, Oct. 27–29, 2008.

14. Hall, S. H. and H. L. Heck, *Advanced Signal Integrity for High-Speed Digital System Design*, Chapter 4, Wiley, Hoboken, NJ, 2009.
15. Chiu, P. W. and G. H. Shiue, "The impact of guard trace with open stub on time-domain waveform in high-speed digital circuits," *2009 IEEE-EPEPS*, 219–212, Portland, OR, Oct. 19–21, 2009.
16. Edwards, T. C. and M. B. Steer, *Foundations of Interconnect and Microstrip Design*, Chapter 7, Wiley, New York, 2000.
17. *Ansoft Designer*, Version 6, Ansoft, Pittsburgh, PA. [Online]. Available: www.ansoft.com.
18. *CST Microwave Studio Manual*, Version 5, Computer Simulation Technology, Germany, [Online]. Available: www.cst.com.
19. Hall, S. H. and H. L. Heck, *Advanced Signal Integrity for High-Speed Digital System Design*, Chapter 4, Wiley, Hoboken, NJ, 2009.